Semiclassical estimation of Franck–Condon factors and transition rates for vertical and nonvertical transitions

A. V. Sergeev and Bilha Segev
Department of Chemistry, Ben-Gurion University of the Negev, POB 653, Beer-Sheva, 84105 Israel

(Received 13 November 2002; accepted 10 January 2003)

We develop a systematic way for estimating multidimensional Franck–Condon factors and transition rates for vertical and nonvertical transitions. By analyzing the phase-space overlap integral, we find the most probable positions and momenta of the nuclei immediately after the electronic transition. We find the transition rate by treating the dominant region in phase space as a funnel for the transition and by calculating the flow of probability through this funnel. We use the Wigner representation and its semiclassical limit and find that the transition occurs through a point(s) on the final surface of constant energy where the initial Wigner function is maximal. This dominant contribution is estimated analytically. Results are illustrated for Harmonic, Morse and Poeschl–Teller oscillators. © *2003 American Institute of Physics.* [DOI: 10.1063/1.1556614]

I. INTRODUCTION: FRANCK–CONDON FACTORS AND TRANSITION RATES

Description of many processes in molecules within an adiabatic (Born–Oppenheimer) framework often involves a Franck–Condon factor, which is defined as a square of the overlap integral between vibrational wave functions belonging to initial and final Born–Oppenheimer surfaces.[1–20]

Franck[21] discovered that the lines in the absorption spectrum of a molecule are the most intense where a classical turning point in the excited state is close to the ground-state equilibrium geometry. Later, Condon generalized Franck's ideas[22] and explained why this was so, using quantum mechanics.[23] The purpose of this study is to develop a new systematic way for estimating the Franck–Condon factors which enter matrix elements that couple different electronic states. We focus here on processes like a radiationless decay in a polyatomic molecule[2,3,6–8,20] when an electronically excited state, usually with a low vibrational energy content, decays into a possibly very large set of almost isoenergetic states, belonging to an underlying electronic term, with a higher degree of vibrational excitation.

There are several methods for calculating Franck–Condon factors; for an overview see Refs. 12, 24–26 and references therein. The straightforward approach of calculating the wave functions and their overlap numerically works well for diatomics yet becomes computationally very demanding for large polyatomic molecules. Different techniques were developed to overcome this difficulty. Among them are methods based on using generating function expansions,[26,27] methods based on sampling the vibrational modes and averaging over typical subgroups of vibration,[28] and semiempirical approaches.[16] Other methods include variational approach,[29] analytical solutions,[30] algebraic approach,[25,31] recursive algorithm,[26] self-consistent field and adiabatic approximations,[32] and perturbation expansion of the potential around the equilibrium.[33] In most of these methods one calculates both the Franck–Condon overlap integrals and the density of final states. The transition rate is then proportional to the absolute value square of an average Franck–Condon integral for different states with the same energy times the density of states at that energy. Our approach differs from these methods in its logic. We first recognize the dominant accepting modes, or more accurately the dominant accepting region in phase space: the most probable positions and momenta of the nuclei immediately after the electronic transition. In particular, we are able to find these positions and momenta in nonvertical as well as vertical transitions. After recognizing the nuclear transition position in phase space we calculate the transition rate by treating the region in phase space found in the first step as a funnel for the transition. We calculate the flow of probability through this funnel. Unlike other methods we do not separate the calculation of Franck–Condon factors from the calculation of the density of final states. Both are calculated together. We note that we do not calculate the strength of the electronic coupling. For complete results for the transition rates these should be estimated through quantum chemistry calculations. In this we do not differ from other methods.

Our approach to Franck–Condon factors is based on a semiclassical approximation in phase space.[34–37] We write the overlap integrals in the Wigner representation[38] and apply an expansion in powers of $\hbar^2$ to the final density matrix.[39–41] The phase-space overlap integral reduces in this way to an integral over the initial Wigner function where the integration is restricted to the final energy surface (leading order) or its close vicinity (next to leading order). In many cases a certain region in phase space dominates. In previous publications[35–37] we developed methods for finding these regions, obtaining in this way propensity rules for energy transfer processes between Born–Oppenheimer surfaces. A mechanistic picture of the transition emerges which we call *surface jumping*: While in vertical electronic transitions the nuclei do not change their positions and momenta, in nonvertical transitions the nuclei *jump*, i.e., change their positions (and) or momenta on the time scale of the electronic transition. One way to think of this mechanism is as an extension and generalization of the well known Tully–Preston surface hopping mechanism.[42] (On surface hopping, see, for

example, Refs. 43–48). While these previous studies demonstrated the concept and provided with some thumb rules for propensities they did not give a systematic way for estimating the *value* of the Franck–Condon integrals. We do so in this paper and compare the results with exact quantum calculations for several different model systems. Below we estimate the value of the integral in terms of the coordinates and momenta at the jumping point, gradients and Hessians of the initial Wigner function and of the final Hamiltonian at this point. The paper is organized in the following way: After reviewing the phase-space approach to Franck–Condon factors in Sec. II we derive the main result of this paper, Eq. (41) for the transition rate, in Sec. III and apply it in Sec. IV to several model examples. These include one-dimensional and two-dimensional anharmonic oscillators and multidimensional harmonic oscillators.

II. FRANCK–CONDON FACTORS AND TRANSITION RATES IN THE WIGNER REPRESENTATION

We would like to find the probability of transition from the initial state of a donor Born–Oppenheimer surface described by the wave function $\psi^{(I)}(\mathbf{q})$ to some state of an acceptor Born–Oppenheimer surface of the energy E_n described by the wave function $\psi_n^{(F)}(\mathbf{q})$ where n is a set of quantum numbers of the final state, and $\mathbf{q}$ is a vector of N components $(q_1,q_2,\ldots,q_N)$. This probability is expressed through the overlap integral between the two wave functions,

$$f_n=\int d\mathbf{q}\psi^{(I)}(\mathbf{q})\psi_n^{(F)}(\mathbf{q}). \tag{1}$$

We are finding the square of this integral averaged over the energies,

$$I(E)=\frac{1}{2\Delta}\sum_{E-\Delta\leqslant E_n\leqslant E+\Delta} f_n^2, \tag{2}$$

where the interval of the averaging $(E-\Delta,E+\Delta)$ is sufficiently narrow in comparison to $|E|$, but sufficiently wide to include many levels of the acceptor. In symbolical operator form, Eq. (2) is rewritten as

$$I(E)=\mathrm{tr}\,\hat{\Pi}^{(I)}\hat{\Pi}_E^{(F)}, \tag{3}$$

$$\hat{\Pi}^{(I)}\equiv|\psi^{(I)}\rangle\langle\psi^{(I)}|, \tag{4}$$

$$\hat{\Pi}_E^{(F)}\equiv\frac{1}{2\Delta}\sum_{E-\Delta\leqslant E_n\leqslant E+\Delta}|\psi_n^{(F)}\rangle\langle\psi_n^{(F)}|. \tag{5}$$

Taking the Wigner transform of Eq. (3), we obtain

$$I(E)=(\pi\hbar)^N\int d\mathbf{q}\,d\mathbf{p}[\hat{\Pi}^{(I)}]_W(\mathbf{q},\mathbf{p})[\hat{\Pi}_E^{(F)}]_W(\mathbf{q},\mathbf{p}), \tag{6}$$

where the Wigner transform of an operator $\hat{A}$ is given by[38]

$$[\hat{A}]_W(\mathbf{q},\mathbf{p})=(\pi\hbar)^{-N}\int d\mathbf{q}'\langle\mathbf{q}+\mathbf{q}'|\hat{A}|\mathbf{q}-\mathbf{q}'\rangle \times\exp(-2i\mathbf{q}'\mathbf{p}/\hbar). \tag{7}$$

The Wigner function of the donor is defined as

$$\rho^{(I)}(\mathbf{q},\mathbf{p})=[\hat{\Pi}^{(I)}]_W(\mathbf{q},\mathbf{p}) =(\pi\hbar)^{-N}\int d\mathbf{q}'\,\psi^{(I)*}(\mathbf{q}+\mathbf{q}') \times\psi^{(I)}(\mathbf{q}-\mathbf{q}')\exp(-2i\mathbf{p}\mathbf{q}'/\hbar). \tag{8}$$

Typically, we consider $\psi^{(I)}$ as the ground-state wave function of a harmonic oscillator,

$$\psi^{(I)}(\mathbf{q})=(\pi\hbar)^{-N/4}\left(\prod_{i=1}^N m_i^{1/2}\omega_i\right)^{1/4} \times\exp\left(-\frac{1}{2\hbar}\sum_{i=1}^N m_i^{1/2}\omega_i q_i^2\right), \tag{9}$$

in which case

$$\rho^{(I)}(\mathbf{q},\mathbf{p})=(\pi\hbar)^{-N}\exp\left(-\frac{2}{\hbar}W(\mathbf{q},\mathbf{p})\right), \tag{10}$$

where

$$W(\mathbf{q},\mathbf{p})=\frac{1}{2}\sum_{i=1}^N (m_i^{-1/2}\omega_i^{-1}p_i^2+m_i^{1/2}\omega_i q_i^2). \tag{11}$$

Generalization to nonharmonic initial states, excited harmonic initial states, or the promoting modes for internal conversion[37] are straightforward. For example, the nth excited state of a one-dimensional harmonic oscillator is exactly given by

$$\rho_n^{(I)}(q,p)=(-1)^n L_n\left(\frac{2m\omega q^2}{\hbar}+\frac{2p^2}{\hbar m\omega}\right) \times\exp\left(-\frac{2}{\hbar}W(q,p)\right), \tag{12}$$

where $W(q,p)$ is given by Eq. (11) with $N=1$ and L_n is the Laguerre polynomial of order n.[49] For a promoting mode q_p we have found in Ref. 37,

$$\rho_{\text{promoting}}^{(I)}(q,p)=\frac{m\omega}{\hbar}\left(\frac{m\omega q^2}{\hbar}+\frac{p^2}{\hbar m\omega}\right) \times\exp\left(-\frac{2}{\hbar}W(q,p)\right) \tag{13}$$

again, with the same $W(q,p)$. The Wigner function of a Morse oscillator is a combination of the modified spherical Bessel function of the third kind (MacDonald function).[49,50] The Wigner function of the ground vibrational state resembles a slightly deformed Gaussian where the close approach side of the function decays more rapidly with an increase of the anharmonicity.[37] Another example is an anharmonic potential with cubic anharmonicities whose ground-state Wigner function was found in Ref. 36. In the following we apply a semiclassical approximation which requires that $\rho^{(I)}(\mathbf{q},\mathbf{p})$ is written in the following form:

$$\rho^{(I)}(\mathbf{q},\mathbf{p})=(\pi\hbar)^{-N}f_0(\mathbf{q},\mathbf{p})\exp\left(-\frac{2}{\hbar}W(\mathbf{q},\mathbf{p})\right). \tag{14}$$

The Wigner function of the acceptor is defined as

$$\rho_E^{(F)}(\mathbf{q},\mathbf{p})=(\pi\hbar)^N[\hat{\Pi}_E^{(F)}]_W(\mathbf{q},\mathbf{p}). \tag{15}$$

The function (15) which is commonly denoted as $[\delta(E-\hat{H}^{(F)})]_W(\mathbf{q},\mathbf{p})$ is approximated in the semiclassical limit as[39–41]

$$\rho_E^{(F)}(\mathbf{q},\mathbf{p})=\delta(E-H^{(F)}(\mathbf{q},\mathbf{p}))+\hbar^2[-f_2\delta''(E-H^{(F)}(\mathbf{q},\mathbf{p}))+f_3\delta'''(E-H^{(F)}(\mathbf{q},\mathbf{p}))], \tag{16}$$

where in the case where the Hamiltonian of the acceptor has the form

$$H^{(F)}(\mathbf{q},\mathbf{p})=\frac{1}{2}\sum_{i=1}^{N}\frac{p_i^2}{m_i}+V^{(F)}(\mathbf{q}), \tag{17}$$

we have

$$f_2=\frac{1}{8}\sum_{i=1}^{N}\frac{1}{m_i}V_{ii}^{(F)''},$$
$$f_3=\frac{1}{24}\sum_{i=1}^{N}\frac{1}{m_i}(V_i^{(F)'})^2+\frac{1}{24}\sum_{i,k=1}^{N}\frac{1}{m_i m_k}V_{ik}^{(F)''}p_i p_k. \tag{18}$$

In Eq. (18), primes denote derivatives with respect to q.

In terms of Wigner functions, Eq. (6) reads

$$I(E)=\int d\mathbf{q}\,d\mathbf{p}\rho^{(I)}(\mathbf{q},\mathbf{p})\rho_E^{(F)}(\mathbf{q},\mathbf{p}). \tag{19}$$

Using approximations (14) and (16) we finally obtain

$$I(E)=I_{f_0}(E)+\hbar^2[-I''_{f_0f_2}(E)+I'''_{f_0f_3}(E)], \tag{20}$$

where for any function $f(\mathbf{q},\mathbf{p})$

$$I_f(E)\equiv(\pi\hbar)^{-N}\int d\mathbf{q}\,d\mathbf{p}f(\mathbf{q},\mathbf{p})\exp\left(-\frac{2}{\hbar}W(\mathbf{q},\mathbf{p})\right)\times\delta(E-H^{(F)}(\mathbf{q},\mathbf{p})), \tag{21}$$

and here primes denote derivatives with respect to E.

III. SEMICLASSICAL ESTIMATION OF THE RATE

A. Estimation of I_f

The integrand in Eq. (21) varies several times in magnitude when the function $W(\mathbf{q},\mathbf{p})$ changes by $\hbar$. We suppose that $\hbar$ is small. Then only a vicinity of one point where $W(\mathbf{q},\mathbf{p})$ is minimal under the constraint $H^{(F)}(\mathbf{q},\mathbf{p})=E$ (and where the integrand is almost maximal) contributes to the integral (21). At this point, that we denote by $(\mathbf{q}^\star,\mathbf{p}^\star)$,

$$\nabla W(\mathbf{q}^\star,\mathbf{p}^\star)=\lambda\nabla H^{(F)}(\mathbf{q}^\star,\mathbf{p}^\star), \tag{22}$$

where λ is an undetermined Lagrange multiplier. Methods for finding the point $(\mathbf{q}^\star,\mathbf{p}^\star)$ analytically for harmonic as well as for some anharmonic potentials and numerically for general potentials are discussed in Refs. 36 and 37.

We use a coordinate system in phase space $\{x_i\}$ with the origin at the point $(\mathbf{q}^\star,\mathbf{p}^\star)$, with the first axis parallel to $\nabla H^{(F)}$, and the 2nd,3rd,...,$2N$th axes perpendicular to $\nabla H^{(F)}$. In practice, we find this coordinate system by Gram–Schmidt orthogonalization of the original basis set of $2N$ unitary vectors parallel to axes q_i and p_i $(i=1,2,...,N)$ with one of the vectors in which direction the function $H^{(F)}$ is the steepest replaced by the vector $\mathbf{n}_1=\nabla H^{(F)}/|\nabla H^{(F)}|$.

We expand W and $H^{(F)}$ in Taylor series around $(\mathbf{q}^\star,\mathbf{p}^\star)$ in this basis set,

$$W=W^\star+W_1x_1+\frac{1}{2}\sum_{i,j=1}^{2N}W_{ij}x_ix_j+\text{cubic and higher order terms}, \tag{23}$$

$$H^{(F)}=H^\star+H_1x_1+\frac{1}{2}\sum_{i,j=1}^{2N}H_{ij}x_ix_j+\text{cubic and higher order terms}, \tag{24}$$

where $W^\star=W(\mathbf{q}^\star,\mathbf{p}^\star)$, $H^\star=H^{(F)}(\mathbf{q}^\star,\mathbf{p}^\star)=E$, $H_1=\partial H^{(F)}/\partial x_1=|\nabla H^{(F)}|$, $W_1=\partial W/\partial x_1=\lambda H_1$, $H_{ij}=\partial^2H^{(F)}/\partial x_i\,\partial x_j$, $W_{ij}=\partial^2W/\partial x_i\,\partial x_j$, and all derivatives are estimated at the point $(\mathbf{q}^\star,\mathbf{p}^\star)$. After substitution of Eqs. (23) and (24) into Eq. (21) and changing variables of integration from x_i to ξ_i where $x_i=\hbar^{1/2}\xi_i$ we obtain the semiclassical limit of $I_f(E)$:

$$I_f(E)\approx\pi^{-N}f^\star\exp\left(-\frac{2}{\hbar}W^\star\right)J(E), \tag{25}$$

where $f^\star=f(\mathbf{q}^\star,\mathbf{p}^\star)$,

$$J(E)=\int d\xi\exp(U(\xi))\,\delta(g(\xi)), \tag{26}$$

and the functions $U(\xi)$ and $g(\xi)$ in Eq. (26) are

$$U(\xi)\equiv-\frac{2}{\hbar}(W-W^\star)=-2\hbar^{-1/2}W_1\xi_1-\sum_{i,j=1}^{2N}W_{ij}\xi_i\xi_j+O(\hbar^{1/2}), \tag{27}$$

$$g(\xi)\equiv H^{(F)}-E=\hbar^{1/2}H_1\xi_1+\frac{\hbar}{2}\sum_{i,j=1}^{2N}H_{ij}\xi_i\xi_j+O(\hbar^{3/2}). \tag{28}$$

We perform first the integration over ξ_1 in Eq. (26),

$$J_1(E,\xi_2,\xi_3,...,\xi_{2N})\equiv\int d\xi_1\exp(U(\xi))\,\delta(g(\xi))=|g_1'(\xi_1^{(0)},\xi_2,\xi_3,...,\xi_{2N})|^{-1}\times\exp(U(\xi_1^{(0)},\xi_2,\xi_3,...,\xi_{2N})), \tag{29}$$

where $\xi_1^{(0)}$ is determined from the equation

$$g(\xi_1^{(0)},\xi_2,\xi_3,...,\xi_{2N})=0. \tag{30}$$

Explicitly,

$$\xi_1^{(0)}=-\frac{\hbar^{1/2}}{2H_1}\sum_{i,j=2}^{2N}H_{ij}\xi_i\xi_j+O(\hbar), \tag{31}$$

and the functions used in Eq. (29) are

$$g_1'(\xi_1^{(0)},\xi_2,\xi_3,...,\xi_{2N})=\hbar^{1/2}H_1+\hbar\sum_{i=2}^{2N}H_{1i}\xi_i+O(\hbar^{3/2}), \tag{32}$$

$$U(\xi_1^{(0)},\xi_2,\xi_3,...,\xi_{2N})=-\sum_{i,j=2}^{2N}F_{ij}\xi_i\xi_j+O(\hbar^{1/2}), \tag{33}$$

where

$$F_{ij}(\mathbf{q},\mathbf{p})=W_{ij}(\mathbf{q},\mathbf{p})-\lambda H_{ij}(\mathbf{q},\mathbf{p}) \tag{34}$$

for $i, j=2,3,...,2N$.

By substitution of Eqs. (32) and (33) into Eq. (29) we find in the leading order in $\hbar$

$$J_1(E,\xi_2,\xi_3,\ldots,\xi_{2N})=\hbar^{-1/2}\frac{1}{H_1}\exp\left(-\sum_{i,j=2}^{2N}F_{ij}\xi_i\xi_j\right). \tag{35}$$

Integrating this Gaussian function over the rest of the $2N-1$ variables in Eq. (26) we find

$$J(E)=\frac{\hbar^{-1/2}}{H_1}\left(\frac{\pi^{2N-1}}{\mathrm{Det}\,\mathbf{F}}\right)^{1/2}. \tag{36}$$

Finally, substituting Eq. (36) into Eq. (25) we find

$$I_f(E)=\frac{f^\star}{H_1}(\pi\hbar\,\mathrm{Det}\,\mathbf{F})^{-1/2}\exp\left(-\frac{2}{\hbar}W^\star\right). \tag{37}$$

Notice that in the leading order in $\hbar$

$$\frac{d^n}{dE^n}I_f(E)=\left(\frac{2}{\hbar}\frac{dW^\star}{dE}\right)^n I_f(E)=\left(\frac{2\lambda}{\hbar}\right)^n I_f(E), \tag{38}$$

where we use the fact that $dW^\star/dE=\lambda$.[36]

B. Estimation of the rate $I(E)$

Since the rate in the tunnelling regime could change by many orders of magnitude, we shall focus here on the logarithm of the rate, namely the quantity of

$$w(E)=-\frac{\hbar}{2}\ln I(E), \tag{39}$$

where the factor $(-\hbar/2)$ is chosen to make $w(E)\approx W^\star$ in the classical limit; see Eq. (40) below.

In the classical limit for the acceptor Wigner function (15) when it is approximated by $\delta(E-H^{(F)}(\mathbf{q},\mathbf{p}))$ [see Eq. (16)] we have $I(E)=I_{f_0}(E)$ [see Eq. (20)]. Hence,

$$w(E)=-\frac{\hbar}{2}\ln I_{f_0}(E)$$

$$\approx W^\star-\frac{\hbar}{2}\ln[(\pi\hbar H_1^2\,\mathrm{Det}\,\mathbf{F})^{-1/2}f_0^\star], \tag{40}$$

where $W^\star$ is the minimum of the function $W(\mathbf{q},\mathbf{p})$ on the surface of constant energy $H^{(F)}(\mathbf{q},\mathbf{p})=E$, $H_1^2=(\nabla H^{(F)}(\mathbf{q}^\star,\mathbf{p}^\star))^2$, and $\mathbf{F}$ is $(2N-1)\times(2N-1)$ matrix of second derivatives of the function $W-\lambda H$ at the point $(\mathbf{q}^\star,\mathbf{p}^\star)$ in directions orthogonal to the gradient $\nabla H^{(F)}(\mathbf{q}^\star,\mathbf{p}^\star)$, see Sec. III. Taking the classical limit $\hbar\to 0$ for the donor Wigner function in Eq. (40), we have simply $w(E)=W^\star$. The second term in Eq. (40) takes into account quasiclassical behavior of the donor Wigner function.

Taking the logarithm of the asymptotic expansion (20) we obtain

$$w(E)=w_0(E)+\hbar^2 w_1(E), \tag{41}$$

where $w_0(E)$ corresponds to the classical limit of the acceptor Wigner function given by Eq. (40), and

$$w_1(E)=\frac{\hbar}{2}[-I''_{f_0f_2}(E)+I'''_{f_0f_3}(E)]/I_{f_0}(E)\approx 4\hbar^{-2}\lambda^3 f_3^\star, \tag{42}$$

where we have used Eqs. (37) and (38) and disregarded the term $I''_{f_0f_2}(E)$ because it is much smaller than $I'''_{f_0f_3}(E)$ in the limit of $\hbar\to 0$.

The expansion (41) is valid (i.e., its second term is much smaller than its leading term, the third term is smaller than the second term, etc.) in the small $\hbar$ limit of the acceptor Wigner function *only*. It is evident from Eqs. (40) and (42) that in the small $\hbar$ limit of the acceptor and donor Wigner functions *simultaneously* the first and the second terms in Eq. (41) have the same order of magnitude with respect to $\hbar$,

$$w_0(E)\sim W^\star,\quad \hbar^2 w_1(E)\sim 4\lambda^3 f_3^\star. \tag{43}$$

Thus, in order to have a valid expansion (41), the acceptor Wigner function should behave in some sense more classically than the donor Wigner function, namely the functions W and $V^{(F)}$ should satisfy

$$4|\lambda^3 f_3^\star|\ll W^\star, \tag{44}$$

where the function W is given by Eq. (11), f_3 is expressed through the potential $V^{(F)}$ according to Eq. (18), and $\lambda=|\nabla W|/|\nabla H^{(F)}|$ at the point $(\mathbf{q}^\star,\mathbf{p}^\star)$. The most important in this criteria is the value of λ which is raised in cube. When the gradient $\nabla H^{(F)}(\mathbf{q}^\star,\mathbf{p}^\star)$ is large, than the criteria (44) is satisfied, and the phase space method is accurate.

Notice that $W(\mathbf{q},\mathbf{0})$ is the same as the classical action $\sigma(\mathbf{q})$ satisfying Hamilton–Jacobi equation $|\nabla\sigma(\mathbf{q})|^2=2(V^{(I)}(\mathbf{q})-V^{(I)}_{\min})$.[42] Taking into account that $W(\mathbf{q},\mathbf{0})$ has zero gradient in direction of momentum,[42] $|\nabla W(\mathbf{q},\mathbf{0})|=[2(V^{(I)}(\mathbf{q})-V^{(I)}_{\min})]^{1/2}$. It means that if the function $V^{(I)}(\mathbf{q})$ is "shallow" and if there is no momentum jump, then $|\lambda|$ is small, and the phase space method is accurate.

If the jumping point $(\mathbf{q}^\star,\mathbf{p}^\star)$ is close to the minimum of the Hamiltonian $H^{(F)}(\mathbf{q},\mathbf{p})$, then $|\nabla H^{(F)}|$ is small, λ is large, and the phase space method diverges.

Finally we note that in the case of several minima of the function $W(\mathbf{q},\mathbf{p})$ on the surface $H^{(F)}(\mathbf{q},\mathbf{p})=E$ with equal or almost the same $W^\star$, all contributions from these points should be summed in order to reproduce the rate $I(E)$. Each of these contributions is given by the formula $\exp(-(2/\hbar)w(E))$ with $w(E)$ approximated by Eq. (41).

In Sec. IV below, we check the inequality (44) and apply the formula for the rate (41) to several model potentials.

IV. COMPARISON WITH EXACT QUANTUM CALCULATIONS

We would like to compare the predictions of the semiclassical method of Eq. (41) with exact quantum calculations of Eq. (2) for some model systems. Before presenting the models and the results, we would like to comment on a subtle point with regard to such a comparison.

As part of the derivation of Eq. (41) we have used Eq. (16) for approximating the acceptor Wigner function by a sum of a δ-function and its derivatives. Rigorously, the expansion in Eq. (16) is valid only in the limit of $\Delta\to 0$, where Δ is the energy interval in the definition of $\hat{\Pi}_E^{(F)}$ by Eq. (5) as

the projector into the subspace of states with energy between $E-\Delta$ and $E+\Delta$. In the limit of $\Delta\to 0$ however, both the acceptor Wigner function, Eq. (15), and the rate, Eq. (19), as functions of the energy E are some linear combinations of δ-functions of the form $\delta(E-E_n)$ where $\{E_n\}$ is the discrete spectrum of the acceptor. There seems to be an inconsistency in approximating $I(E)$ which is strictly speaking a sum of δ-functions by Eq. (20) which sums over smooth analytic functions of E. To understand this apparent inconsistency, let us review the derivation of the expansion of Eq. (16) as it was done in Ref. 40. First it was proven that

$$[e^{-i\hat{H}^{(F)}\tau}]_W(\mathbf{q},\mathbf{p})=\hbar^{-N}e^{-iH^{(F)}(\mathbf{q},\mathbf{p})\tau}[1+\hbar^2(f_2(\mathbf{q},\mathbf{p})\tau^2 - if_3(\mathbf{q},\mathbf{p})\tau^3)+\cdots]. \tag{45}$$

Notice that at this step both sides of Eq. (45) are smooth analytic functions of the parameter τ. To derive the expansion over $\hbar^2$ for the function $[\delta(E-\hat{H}^{(F)})]_W(\mathbf{q},\mathbf{p})$, Eq. (45) is considered as a Fourier-component of this function, so Eq. (16) is derived by applying the inverse Fourier transform to Eq. (45) with respect to the parameter τ. During this derivation it is implicitly assumed that the expansion (45) is valid uniformly with respect to τ. We can see, however, from Eq. (45) that the first correction grows with τ, so at least higher Fourier components of Eq. (16) could not be expanded in power series in $\hbar^2$. As a result, Eq. (16) has sense for a discrete spectrum only if we shield these higher Fourier components, applying some method of smoothing or averaging to the exact discrete formula for the rate. Several options for such smoothing are suggested in the Appendix.

Below we consider one-dimensional examples where the donor potential is a harmonic oscillator, and the acceptor potential is Morse or Poeschl–Teller oscillators, two-dimensional examples with a combination of Morse and harmonic oscillators which involve a Duchinsky rotation, and multidimensional harmonic oscillators.

A. First model: Transitions from a harmonic oscillator into a Morse oscillator in one dimension

Suppose that the initial and final Hamiltonians are given, respectively, by:

$$H^{(I)}(q,p)=\tfrac{1}{2}p^2+\tfrac{1}{2}\omega^2q^2, \tag{46}$$

$$H^{(F)}(q,p)=\tfrac{1}{2}p^2+\tfrac{1}{2}(J+\tfrac{1}{2})(1-e^{-\beta q})^2, \tag{47}$$

where ω is the frequency of the harmonic oscillator, $m=1$, $\beta=(J+\frac{1}{2})^{-1/2}$, and in the numerical example below $J=300$ is the number of bound states in the Morse potential.

The ground-state wave function of the harmonic oscillator is

$$\psi^{(I)}(q)=(\omega/\pi)^{1/4}\exp(-\tfrac{1}{2}\omega q^2). \tag{48}$$

Eigenfunctions of the Schrödinger equation for the Morse oscillator are expressed in terms of the associated Laguerre polynomials[51]

$$\psi_n^{(F)}(q)=C_n^{-1/2}\exp(-\tfrac{1}{2}\xi)\xi^{J-n}L_n^{2(j-n)}(\xi), \tag{49}$$

$$E_n=n+\tfrac{1}{2}-(2J+1)^{-1}(n+\tfrac{1}{2})^2, \tag{50}$$

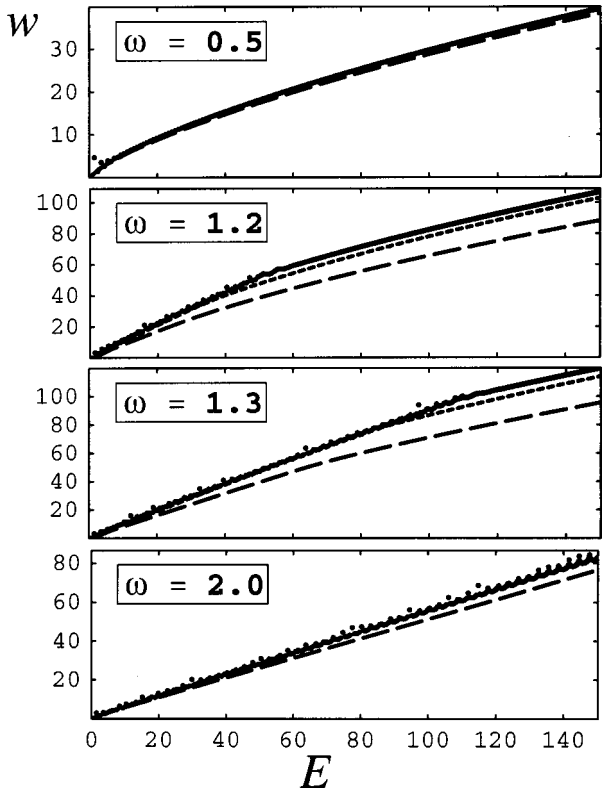

FIG. 1. The function $w(E)$ found by numerical integration over the exact wave functions at points of the discrete spectrum, $E=E_n$, $n=0,1,...,J-1$ (dots) and results of the estimation of the phase-space integral (dashed and dotted lines) for one-dimensional Hamiltonians. The donor Hamiltonian is a harmonic oscillator given by Eq. (46) and the acceptor Hamiltonian is a Morse oscillator given by Eq. (47). The dashed line represents the leading order approximation, and the dotted line includes next to leading order corrections. For $\omega=0.5$ and $\omega=2.0$ the dotted line is practically indistinguishable from the exact results for most of the energies.

where $C_n=[2\beta(J-n)n!]^{-1}(2J-n)!$ and $\xi=(2J+1)e^{-\beta q}$. We use here atomic units with $\hbar=1$. Performing numerical integration in Eq. (1) and using Eqs. (2) and (39), we determine the function $w(E)$, which is defined as the logarithm of the transition rate obtained from the exact quantum calculations. We used $\Delta=\frac{1}{2}dE_n/dn$, in which case the sum in Eq. (2) has one term, and

$$w(E_n)=-\tfrac{1}{2}\ln[(dE_n/dn)^{-1}f_n^2]. \tag{51}$$

Results are shown in Fig. 1 by dots, corresponding to $n=0,1,...,J-1$. Results of averaging over the discrete rate as described in the Appendix are shown by solid lines that usually overlap with the discrete points of $w(E_n)$.

Our analysis of the phase space integral starts from finding all stationary points of the function $W(q,p)=\frac{1}{2}(p^2/\omega+\omega q^2)$ subject to the constraint $H^{(F)}(q,p)=E$. Generally there are six stationary points,

$$(q_L,0),(q_R,0),\quad (0,p_E),(0,-p_E),\quad (\overline{q},\overline{p_E}),(\overline{q},-\overline{p_E}), \tag{52}$$

where the turning points q_L and q_R are negative and positive roots of the equation $V^{(F)}(q)=E$, $p_E=(2E)^{1/2}$, $\overline{q}$ is a root of the equation $V'^{(F)}(q)/q=\omega^2$, and $\overline{p_E}=[2(E-\overline{E})]^{1/2}$ with $\overline{E}=V^{(F)}(\overline{q})$. The last two stationary points exist only if E

$>\overline{E}$. For each stationary point we calculated the second derivative in phase space of the Hamiltonian in a direction orthogonal to its gradient and multiplied it by the square of the gradient, and obtained

$$G=(H_q^{(F)})^2F_{pp}+(H_p^{(F)})^2F_{qq}-2H_q^{(F)}H_p^{(F)}F_{qp}, \tag{53}$$

where $F(q,p)=W(q,p)-\lambda H^{(F)}(q,p)$, $H_q=\partial H/\partial q$, $H_p=\partial H/\partial p$, $F_{pp}=\partial^2F/\partial p\,\partial p$, $F_{qq}=\partial^2F/\partial q\,\partial q$, $F_{qp}=\partial^2F/\partial q\,\partial p$, and all derivatives are estimated at the point $(\mathbf{q}^\star,\mathbf{p}^\star)$. Each point with a positive G is a local minimum and thus contributes to the integral $I_1(E)$ a term of the form

$$(\pi G)^{-1/2}\exp(-2W(q,p)) \tag{54}$$

and a similar term to the quasiclassical correction calculated using Eq. (42). In fact, only one stationary point or a symmetric pair give the dominant contribution. Results for $w_0(E)$ and $w_0(E)+w_1(E)$ are shown in Fig. 1 by dashed and dotted lines, respectively.

We found that the correction to the integral $I_1(E)$ is small and our estimations are accurate if the two potentials, the donor and acceptor, considerably differ. In this model we have scaled the potential $V^{(F)}$ so that the frequency of small vibrations is one, and varied the frequency ω of the potential $V^{(I)}$. Thus, the results are accurate if ω is small or large. We have found that if $\omega\leqslant 0.5$ or $\omega\geqslant 2$ our results including the first correction (dotted lines) are practically indistinguishable from the exact quantum calculations.

Finally we notice that if $\omega=1$ then Eq. (37) is not applicable because surfaces of equal $H^{(F)}$ and equal W have equal second derivatives and $\mathrm{Det}\,\mathbf{F}=0$. In this case the integrals could be found in principle by direct numerical integration of Eq. (21). This apply as well to the example of the next model.

B. Second model: Transitions from a harmonic oscillator into a Poeschl–Teller oscillator in one dimension

For the second example, the initial Hamiltonian $H^{(I)}(q,p)$ is given by Eq. (46) and the final Hamiltonian is

$$H^{(F)}(q,p)=\tfrac{1}{2}p^2-\tfrac{1}{2}\alpha^{-2}(\cosh^{-2}\alpha q-1), \tag{55}$$

where $\alpha=[J(J+1)]^{-1/4}$ and in the numerical example below $J=400$ is the number of bound states in the Poeschl–Teller potential. Here we are interested only in even parity states with nonzero overlap integral.

The eigenfunctions of the Schrödinger equation for the Poeschl–Teller oscillator are expressed in terms of the hypergeometric functions[52]

$$\psi_n^{(F)}(q)=C_n^{-1/2}\chi_n(q), \tag{56}$$

$$\chi_n(q)=(1+\xi)^{(J+1)/2}{}_2F_1(\tfrac{1}{2}(n+1),\tfrac{1}{2}(2J-n+1);\tfrac{1}{2};-\xi), \tag{57}$$

$$E_n=-\tfrac{1}{2}\alpha^2(J-n)^2+\tfrac{1}{2}\alpha^{-2}, \tag{58}$$

where $C_n=\int_{-\infty}^{\infty}\chi_n^2(q)dq$ and $\xi=\sinh^2\alpha q$.

Figure 2 shows the results of the exact quantum mechanical numerical integration calculated and depicted in the same way as in the previous subsection. The analysis of the phase-space integral is also done in a similar way to the previous subsection. Here, the last pair of stationary points in Eq. (52) does not exist for $\omega>1$, and is replaced by a quartet of points $(\pm\overline{q},\pm\overline{p_E})$ if $\omega<1$. The results displayed in Fig. 2 show that the correction to the integral $I_1(E)$ is small, and our estimations are accurate if ω is small or large. The first correction $w_1(E)$ sometimes exhibit a discontinuous derivative (spike) because of a competition between different local minima. Around these spikes the approximation is usually less accurate, and sometimes completely inadequate. [In the worst case for $\omega=0.2$ and $E=184$ there is an error of ≈ 30 in w corresponding to an error by a factor of $\sim 10^{30}$ times in $I(E)$.]

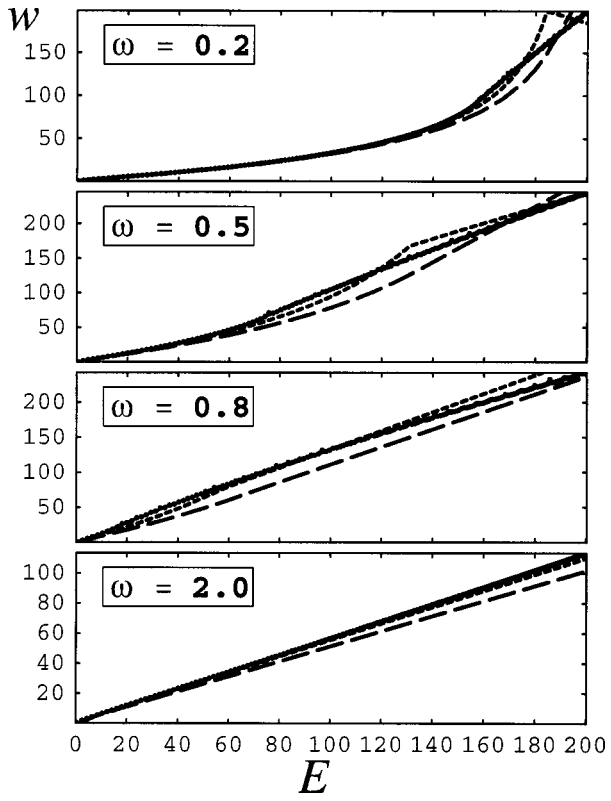

FIG. 2. The same as for Fig. 1 but for the acceptor Hamiltonian of Poeschl–Teller oscillator given by Eq. (55).

C. Third model: Transitions from a harmonic oscillator into a combination of a Morse oscillator and a harmonic oscillator in two dimensions

Here we consider an example in two dimensions, (q_1,q_2), where the initial and final potentials, respectively, are,

$$V^{(I)}(\mathbf{q})=\tfrac{1}{2}\omega_1'^2(\cos\phi q_1+\sin\phi q_2)^2+\tfrac{1}{2}\omega_2'^2(-\sin\phi q_1+\cos\phi q_2)^2, \tag{59}$$

$$V^{(F)}(\mathbf{q})=\tfrac{1}{2}(J+\tfrac{1}{2})[1-\exp(-(J+\tfrac{1}{2})^{-1/2}q_1)]^2+\tfrac{1}{2}\omega_2^2q_2^2. \tag{60}$$

The initial Hamiltonian, $H^{(I)}(\mathbf{q},\mathbf{p})=\tfrac{1}{2}\mathbf{p}^2+V^{(I)}(\mathbf{q})$, is a Hamiltonian of a separable anisotropic harmonic oscillator with well known eigenfunctions. The final Hamiltonian,

TABLE I. Comparison of exact quantum calculation of the rate $w(E)$ with the semiclassical approximation of Eqs. (40) and (41) for the two-dimensional model potentials given by Eqs. (59) and (60). $w_0(E)$ is the leading-order phase-space approximation while w_0+w_1 includes the next to leading order correction. For these examples, we chose $J=300$ and $E=100$. ω_1', ω_2', ϕ, and ω_2 are parameters of the model. In particular ϕ is the Duchinsky rotation angle. $(q_1^\star,q_2^\star,p_1^\star,p_2^\star)$ and $W^\star$ are the coordinates, momenta, and logarithm of the initial Wigner function at the jumping point.

No.	ω_1'	ω_2'	ϕ	ω_2	$q_1^\star$	$q_2^\star$	$p_1^\star$	$p_2^\star$	$W^\star$	λ	$w_0(E)$	w_0+w_1	$w(E)$
1	0.2	1	$\pi/3$	1	−7.44	−10.66	0	0	17.40	0.158	19.344	19.553	19.572
2	0.2	1	$\pi/6$	1	−9.86	−4.86	0	0	12.29	0.096	14.486	14.572	14.578
3	1	2	$\pi/4$	2	−3.17	−6.85	0	0	31.90	0.317	33.21	37.37	38.64
4	3	7	$\pi/4$	1	0	0	10.00	−10.00	14.29	0.143	15.879	15.976	15.979
5	3	7	$\pi/4$	5	0	0	10.00	−10.00	14.29	0.143	15.40	16.67	16.84

$H^{(F)}(\mathbf{q},\mathbf{p})=\frac{1}{2}\mathbf{p}^2+V^{(F)}(\mathbf{q})$, is also separable. Its eigenstates are products of Morse oscillator eigenfunctions of the variable q_1 numbered by the quantum number n_1 and harmonic oscillator eigenfunctions of the variable q_2 numbered by the quantum number n_2 with the energy eigenvalues $E_{n_1,n_2}=n_1+\frac{1}{2}-(2J+1)^{-1}(n_1+\frac{1}{2})^2+\omega_2(n_2+\frac{1}{2})$. We have found the exact quantum mechanical overlap integrals numerically for different quantum numbers, and the rate $I(E)$ by averaging over the squares of these overlap integrals by the method of Eq. (A6) as described below in the Appendix.

We have applied the phase-space method to this model in the following way. To find the stationary points of the function $W(\mathbf{q},\mathbf{p})$ under the constraint $H^{(F)}(\mathbf{q},\mathbf{p})=E$, we have used the fact that for large J the final potential is almost harmonic, $V^{(F)}(\mathbf{q})\approx\frac{1}{2}q_1^2+\frac{1}{2}\omega_2^2q_2^2$. In this limit all the stationary points are determined by the method described in Ref. 36. Then, by decrementing J and continuously tracing all stationary points, we determine them for finite J. Functions $w_0(E)$ and $w_1(E)$ are finally found as described above in Sec. III B. Results for several parameters of the potentials of Eqs. (59) and (60) are shown in Table I. Examples 1, 2, and 4 have small w_1 and demonstrate excellent convergence of the expansion of Eq. (41), examples 3 and 5 show slower convergence. Examples 1, 2, and 3 have the dominant point $(\mathbf{q}^\star,\mathbf{p}^\star)$ in phase space with $\mathbf{q}^\star\neq 0$ and $\mathbf{p}^\star=0$ (exhibiting a coordinate jump), and examples 4 and 5 have $\mathbf{q}^\star=0$ and $\mathbf{p}^\star\neq 0$ (exhibiting a momentum jump). For more details of the location of the jumping point $(\mathbf{q}^\star,\mathbf{p}^\star)$, see Fig. 3.

D. Fourth model: Transitions between multidimensional harmonic oscillators

The previous examples have demonstrated that the method works well for anharmonic potentials, and for cases with considerable Duchinsky rotation. Our purpose here is to demonstrate that it can be applied as well to large polyatomic molecules. We therefore choose a ten-dimensional oscillator. For simplicity, we consider the multidimensional harmonic oscillator model:

$$H^{(I)}(\mathbf{q},\mathbf{p})=\frac{1}{2}\sum_{k=1}^{N}[p_k^2+\omega_k^2(q_k-a_k)^2],$$

$$H^{(F)}(\mathbf{q},\mathbf{p})=\frac{1}{2}\sum_{k=1}^{N}(p_k^2+q_k^2). \tag{61}$$

Here, the initial Hamiltonian is an anisotropic oscillator with a shifted minimum, and the final Hamiltonian is an isotropic oscillator with frequency equal to one. The final energy is $E_n=n+N/2$ where $n=n_1+n_2+\ldots+n_N$ is a sum of the quantum numbers of the individual one-dimensional oscillators. A two-dimensional version of this model was studied in Ref. 35 and in Ref. 36 where we considered, respectively, propensities for different excitations and relation to classical trajectories. We did not calculate transition rates. We do so here for the multidimensional case.

Since the spacing of the final energy spectrum is one, the rate averaged over the energy is a sum of rates of transition to individual states comprising a manifold of degenerate states with the quantum number n,

$$I^{(N)}(E_n)=\sum_{n_1+n_2+\ldots+n_N=n} f_{n_1}^{(1)^2}f_{n_2}^{(2)^2}\ldots f_{n_N}^{(N)^2}, \tag{62}$$

where $f_{n_k}^{(k)}$ are one-dimensional overlap integrals between the ground-state wave function of the harmonic oscillator $\frac{1}{2}[p_k^2+\omega_k^2(q_k-a_k)^2]$ and the excited state wave function with the quantum number n_k of the Hamiltonian $\frac{1}{2}(p_k^2+q_k^2)$.

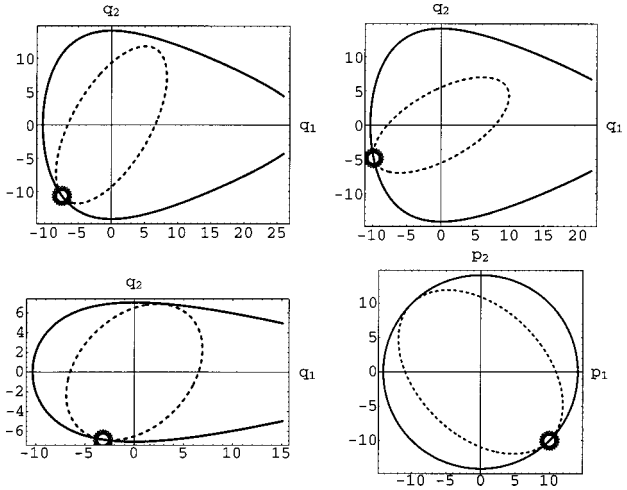

FIG. 3. The figure displays coordinate-space or momentum-space cuts through the surface defined by $H^{(F)}(\mathbf{q},\mathbf{p})=E$ (solid line) and the tangent surface of constant $W(\mathbf{q},\mathbf{p})$ (dotted line) for the two dimensional model of Sec. IV C. The potentials are given by Eqs. (59) and (60) each time with different parameters as in the examples 1–5 from Table I, starting from top left, and ending at the bottom right. (The last figure fits both examples 4 and 5.) The point of contact between the surface defined by $H^{(F)}(\mathbf{q},\mathbf{p})=E$ and the tangent surface of constant $W(\mathbf{q},\mathbf{p})$ is the jumping point $(\mathbf{q}^\star,\mathbf{p}^\star)$ marked by a circle. The overlap integral is estimated by the flow of probability through this point with very good agreement with the exact numerical results.

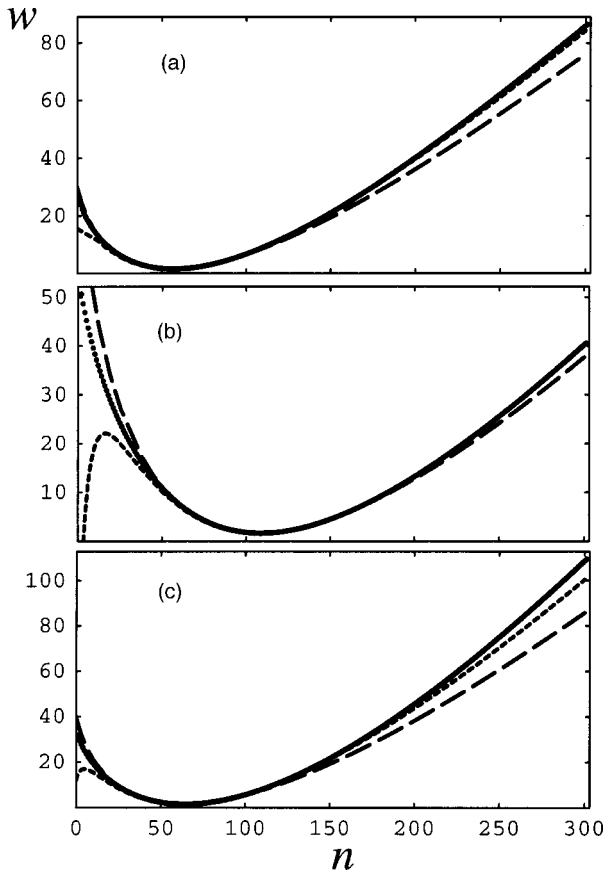

FIG. 4. The logarithm of the transition rate $w(E_n)=-\frac{1}{2}\ln I(E_n)$ as a function of the quantum number n for the N-dimensional model of harmonic oscillators described by Eq. (61). All the parameters of the examples (a), (b), and (c) are listed in Table II. Dots (often overlapping) are the results of exact quantum calculations, the dashed and dotted lines are the results of estimation of the phase space integral using Eq. (40) and the more accurate Eq. (42), respectively.

Exact quantum calculations were made with frequencies $\omega_k=\omega_{\max}\alpha_k$ and displacements $a_k=a_{\max}\beta_k$, where α_k and β_k are numbers randomly distributed in the interval $[-1,1]$. The results are shown in Fig. 4 for the randomly chosen parameters listed in Table II. The minimum of the curves $w_{\min}\approx 0$ corresponds to an allowed or vertical transition where $V^{(F)}(\mathbf{a})=E_n$ which occurs at

$$n=n_{\min}=(|\mathbf{a}|^2-N)/2. \tag{63}$$

We want to compare the exact quantum results to results obtained within the semiclassical phase-space approximation. To do so we first find the point $(\mathbf{q}^\star,\mathbf{p}^\star)$ using the method[36] for a general system of harmonic oscillators. Namely, we find λ as the smallest root of the equation

$$\frac{1}{2}\sum_{i=1}^{2N}\left(\frac{\lambda_i}{\lambda_i-\lambda}\right)^2 X_i^2=E, \tag{64}$$

where $\lambda_n=\omega_n$, $\lambda_{N+n}=1/\omega_n$, $X_n=a_n$, and $X_{N+n}=0$ for $i=1,2,...,N$. Here we suppose for simplicity that there is only one "preferable direction of jump," or among the numbers $\{\lambda_1,\lambda_2,\ldots,\lambda_{2N}\}$ there is one smallest number λ_{i_0}, and $X_{i_0}\neq 0$ (the general case is considered in Ref. 36). For this case, as was proven in Ref. 36 the components of the vector $\mathbf{x}^\star=(\mathbf{q}^\star,\mathbf{p}^\star)$ are given by

$$x_i^\star=\frac{\lambda_i}{\lambda_i-\lambda}X_i. \tag{65}$$

Then, the approximation $w_0(E)$ and the correction $\hbar^2 w_1(E)$, Eqs. (40) and (42), are easily expressed through λ and $x_i^\star$ as

$$w_0(E)=\frac{1}{2}\sum_{i=1}^{2N}\lambda_i(x_i^\star-X_i)^2 + \frac{\hbar}{4}\ln\left(\pi\hbar\prod_{i=1}^{2N}(\lambda_i-\lambda)\sum_{i=1}^{2N}\frac{x_i^{\star 2}}{\lambda_i-\lambda}\right), \tag{66}$$

$$\hbar^2 w_1(E)=\tfrac{1}{6}\lambda^3|\mathbf{x}^\star|^2. \tag{67}$$

If the displacements are small, then $\lambda\to\lambda_{i_0}$, $w_0(E)\approx\frac{1}{2}\lambda^2\lambda_{i_0}X_{i_0}^2(\lambda_{i_0}-\lambda)^{-2}$, $\hbar^2 w_1(E)\approx\frac{1}{6}\lambda^3\lambda_{i_0}^2X_{i_0}^2(\lambda_{i_0}-\lambda)^{-2}$, and the condition (44) is equivalent to $\hbar^2 w_1/w_0\approx\frac{1}{3}\lambda\lambda_{i_0}\approx\frac{1}{3}\lambda_{i_0}^2\ll 1$. It means that either the smallest among the frequencies $\{\omega_1,\omega_2,\ldots,\omega_N\}$ is much smaller than one or the largest frequency is much larger then one. When the frequencies of the initial potential are close to the frequency of the final potential (which here is one), the rate is generally smaller (w is larger), and the phase space method is less accurate, see panel (c). A small n corresponds to a jumping point $(\mathbf{q}^\star,\mathbf{p}^\star)$ which is close to the minimum of $H^{(F)}(\mathbf{q},\mathbf{p})$ where the phase-space method does not work, see discussion of the criteria of applicability (44) in Sec. III B.

V. CONCLUSIONS

Surface jumping is an intuitive concept. It gives a simple mechanistic picture of radiative or radiationless transitions between potential energy surfaces. According to this picture immediately after an electronic transition the nuclei are at a well defined region in phase space. Here we have shown that

TABLE II. Parameters (frequencies and displacements) of the examples of ten-dimensional harmonic oscillator (61) for which we performed numerical experiments, see Fig. 4. The quantum number $n_{\min}$, Eq. (63), corresponding to a vertical transition, is 51.33, 102.92, and 58.76 for Figs. 4(a), 4(b), and 4(c), respectively.

Figure	Parameter	$n=1$	2	3	4	5	6	7	8	9	10
4a	ω_n	0.95	0.83	0.98	1.42	0.52	0.64	0.73	0.73	1.79	0.76
	a_n	−2.23	3.52	−4.83	3.31	−1.54	2.75	4.94	−2.07	0.71	−4.68
4b	ω_n	0.90	0.52	0.62	0.59	1.62	1.60	0.59	0.52	1.44	1.31
	a_n	3.42	6.94	−3.62	−4.08	−6.93	4.22	−4.04	−0.68	−6.11	−2.48
4c	ω_n	0.86	0.95	1.11	0.94	1.04	0.89	1.11	0.96	1.05	0.95
	a_n	4.58	2.47	−4.82	4.61	4.72	0.46	2.57	4.51	−1.60	2.02

when this simple picture applies, the transition rate can be calculated from the flow of probability from one potential energy surface to another at that phase-space region. We have derived Eqs. (40) and (42) as successive approximation for this rate and compared the results obtained from this formulas with exact quantum calculations for several models. The agreement is very good as long as the accepting potential at the jumping point is steep enough and as long as the jumping point location is not too sensitive to the parameters of the problem.

The method is not restricted to these examples and could be applied in general to multidimensional anharmonic systems with relative ease. The reason we choose these models here is that for them an exact quantum calculations is possible thus allowing for a comparison. The exact quantum calculations of anharmonic Franck–Condon factors become very difficult with higher dimension while our methods scale very well. Errors of our method for predicting the logarithm of the transition rate, seem to scale at worst linearly with the dimension of the problem.

Future work will include application to specific polyatomic molecules and comparison with experimental results.

It is interesting to compare our approach to another semiclassical technique for the calculation of electronic transition rates.[53] Weide and Schinke analyze structures in the absorption band of water by means of classical trajectories on a single surface. While they study motion on a single potential energy surface and neglect the nonadiabatic coupling between different surfaces, we study the direct transition between surfaces, neglecting subsequent motion on the accepting surface. Future work may aim at combining these complementary treatments by using the jump as initial conditions for motion on the accepting surface.

ACKNOWLEDGMENTS

This research was supported by a grant from the United States-Israel Binational Science Foundation (BSF), Jerusalem, Israel. We are grateful to Professor E. J. Heller for many useful discussions.

APPENDIX: DIFFERENT WAYS FOR AVERAGING THE EXACT RATE OVER A DISCRETE SPECTRUM

In this Appendix we discuss several methods for averaging over the discrete values of the exact quantum rate. The averaging is necessary in order to compare the results of the exact quantum calculations with predictions of the semiclassical formula (20) that intrinsically averages over an energy window.

The discrete formula for the rate is:

$$I_{\mathrm{discr}}(E)\equiv I^{(\Delta\to 0)}(E)=\sum_n I_n\delta(E-E_n), \tag{A1}$$

where I_n is the square of the overlap integral f_n given by Eq. (1) that could be found in principle by solving the Schrödinger equation with subsequent integration over $\mathbf{q}$.

The simplest method of smoothing the function $I_{\mathrm{discr}}(E)$ is its averaging over a rectangular energy window defined by the interval $[E-\Delta,E+\Delta]$,

$$\tilde{I}(E)=\frac{1}{2\Delta}\int_{E-\Delta}^{E+\Delta} I_{\mathrm{discr}}(E')dE', \tag{A2}$$

where the interval $[E-\Delta,E+\Delta]$ contains at least one level of the discrete spectrum. Obviously, the definition of Eq. (A2) is identical to our original definition of the rate $I(E)$ with $\Delta\neq 0$; see Eq. (2). A disadvantage of this method of smoothing is that $\tilde{I}(E)$ still remains a discontinuous function of the variable E.

As an alternative, let us consider smoothing by integration with a Gaussian energy window,

$$\begin{aligned}\tilde{I}_0(E)&=\frac{M_0}{\pi^{1/2}\Delta},\\ M_0&=\int \exp\left(-\frac{(E'-E)^2}{\Delta^2}\right)I_{\mathrm{discr}}(E')dE'.\end{aligned} \tag{A3}$$

This method replaces the sum over δ-functions in Eq. (A1) by a sum over Gaussian functions. If the width Δ is larger than the spacing of the spectrum, we could expect good smoothing. There is some disadvantage however to use too large Δs because the smoothing distorts some regularly behaving but nonconstant functions. For large energy gaps or for small displacements of the Born–Oppenheimer surfaces, the rate behaves typically as $f_0e^{\alpha E}$.[1] In this case the smoothing by Eq. (A3) overestimates the rate because $\tilde{I}_0(E)=f_0\exp(\alpha E+\alpha^2\Delta^2/4)$.

An improved Gaussian smoothing can be defined as

$$\tilde{I}_1(E)=\frac{M_0}{\pi^{1/2}\Delta}\exp(-(M_1/M_0)^2), \tag{A4}$$

where the moments M_n are defined as

$$M_n=\int\left(\frac{E'-E}{\Delta}\right)^n\exp\left(-\frac{(E'-E)^2}{\Delta^2}\right)I_{\mathrm{discr}}(E')dE'. \tag{A5}$$

This method allows to use larger widths Δ for averaging, because it does not distort so much regular behavior of the rate as does method (A3). It does not change functions of the form $\sim f_0e^{\alpha E}$, but it still slightly changes functions of a more general but still quite typical form $\sim f_0\exp(\alpha E+\beta E^2)$.

Refining further Eq. (A4), we arrive at the formula

$$\tilde{I}_2(E)=\frac{M_0^2}{\pi^{1/2}\Delta D}\exp\left(-\frac{M_1^2}{D^2}\right),\quad D=[2(M_0M_2-M_1^2)]^{1/2}. \tag{A6}$$

This method correctly reproduces behavior of $\sim f_0\exp(\alpha E+\beta E^2)$ without distortions even for large Δ.

We tested the different methods of averaging to find a continuous analogue of the discrete rate I_{discr} for a number of potentials discussed in Sec. IV. We found that with an increase of the interval of averaging the logarithms of $\tilde{I}_0$, $\tilde{I}_1$, and $\tilde{I}_2$ typically oscillate for small Δ, have a shallow plateau at some intermediate Δ_0, and change polynomially for large

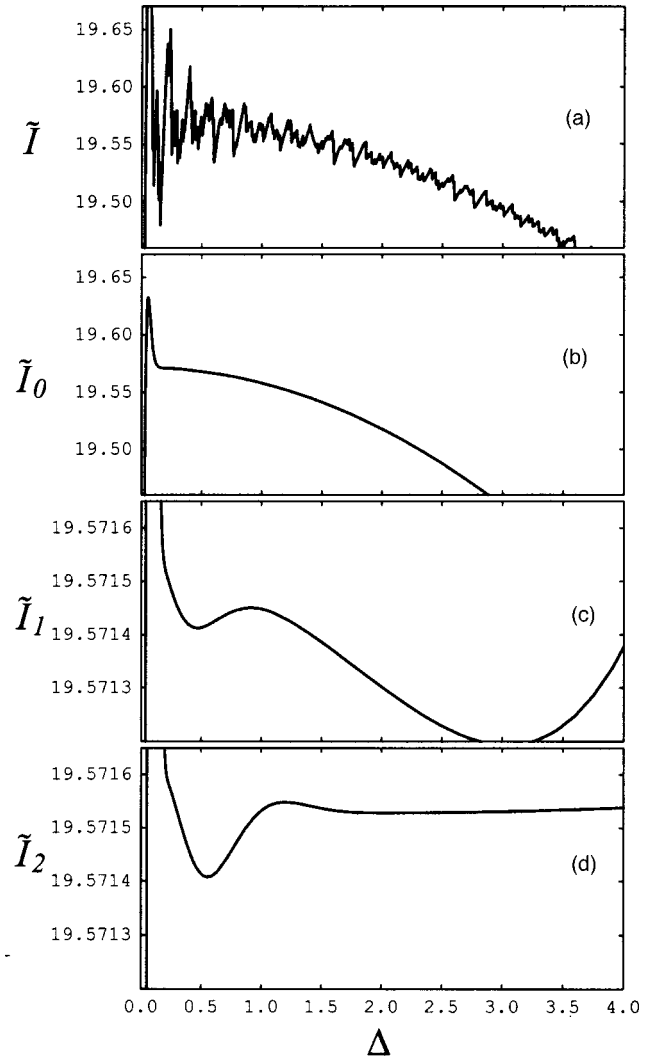

FIG. 5. Smoothing of the rate $I_{\mathrm{discr}}(E)$ for a discrete spectrum using different methods and different intervals of averaging. For this example, the Hamiltonians of the donor and acceptor are $H^{(I)}=p_x^2/2+p_y^2/2+1/50(19x^2-12\sqrt{3}xy+7y^2)$ and $H^{(F)}=p_x^2/2+p_y^2/2+\frac{1}{2}(J+\frac{1}{2})\ [1-\exp(-(J+\frac{1}{2})^{-1/2}x)]^2+\frac{1}{2}y^2$ with $J=300$, and $E_0=100$. Since the energy E_0 does not coincide with any discrete level, $I_{\mathrm{discr}}(E_0)=0$. However, there are many levels close to E_0 (the closest ones are $E_{(n_x=0,n_y=99)}=99.9996$ and $E_{(n_x=24,n_y=76)}=100.0112$), so we expect that the smoothed rate $\tilde{I}(E_0)\neq 0$ if the width of the energy band $\Delta>0.0004$. The graphs show $-\hbar/2$ of the logarithm of the rate as a function of Δ for four different methods of averaging given by Eqs. (A2), (A3), (A4), and (A6), see panels (a), (b), (c), and (d) respectively. Here we set $\hbar=1$. The semiclassical approximation gives $w_0(E_0)=19.344$, $w_0(E_0)+\hbar^2 w_1(E_0)=19.553$. The last result is close to the plateaus of the curves.

Δ, as demonstrated for some examples in Fig. 5. The optimal $\Delta=\Delta_0$ corresponding to the plateau is numerically determined by minimizing the averaged absolute value of the derivative, $1/\Delta_0\int_{\Delta_0}^{2\Delta_0}|dw_\Delta(E)/d\Delta|d\Delta$, while the optimized average rate is determined as the averaged value near $\Delta=\Delta_0$, $w_{\mathrm{opt}}(E)=1/\Delta_0\int_{\Delta_0}^{2\Delta_0}w_\Delta(E)d\Delta$. We found that the most shallow minimum and the most accurate result of averaging is achieved with use of the method of $\tilde{I}_2$.

[1] W. Siebrand, J. Chem. Phys. **46**, 440 (1967).
[2] M. Bixon and J. Jortner, J. Chem. Phys. **48**, 715 (1968).
[3] S. A. Rice, I. McLaughlin, and J. Jortner, J. Chem. Phys. **49**, 2756 (1968).
[4] S. E. Nielsen and R. S. Berry, Chem. Phys. Lett. **2**, 503 (1968).
[5] R. S. Berry and S. E. Nielsen, J. Chem. Phys. **49**, 116 (1968).
[6] M. Bixon and J. Jortner, J. Chem. Phys. **50**, 4061 (1969).
[7] J. Jortner, S. A. Rice, and R. M. Hochstrasser, Adv. Photochem. **7**, 149 (1969).
[8] J. Jortner, J. Chim. Phys. Phys.-Chim. Biol. , p. 9 (1969).
[9] R. S. Berry and S. E. Nielsen, Phys. Rev. A **1**, 383 (1970).
[10] R. S. Berry and S. E. Nielsen, Phys. Rev. A **1**, 395 (1970).
[11] R. Englman, *The Jahn-Teller Effect in Molecules and Crystals* (Wiley Interscience, London, 1972).
[12] W. Domcke, L. S. Cederbaum, H. Köppel, and W. Von Niessen, Mol. Phys. **34**, 1759 (1977).
[13] R. Englman, *Non-radiative Decay of Ions and Molecules in Solids* (North-Holland, Amsterdam, 1979).
[14] E. S. Medvedev, Chem. Phys. **73**, 243 (1982).
[15] G. Fischer, *Vibronic Coupling* (Academic, London, 1984).
[16] V. I. Osherov and E. S. Medvedev, Opt. Spectrosc. **67**, 53 (1989).
[17] E. S. Medvedev, Theor. Math. Phys. **90**, 146 (1992).
[18] E. E. Nikitin and L. P. Pitaevskii, Phys. Usp. **36**, 851 (1993).
[19] E. E. Nikitin and L. P. Pitaevskii, Phys. Rev. A **49**, 695 (1994).
[20] E. S. Medvedev and V. I. Osherov, *Radiationless Transitions in Polyatomic Molecules* (Springer, Berlin, 1995).
[21] J. Franck, Trans. Faraday Soc. **21**, 536 (1925).
[22] E. Condon, Phys. Rev. **28**, 1182 (1926).
[23] E. U. Condon, Phys. Rev. **32**, 858 (1928).
[24] P.-Å. Malmqvist and N. Forsberg, Chem. Phys. **228**, 227 (1998).
[25] T. Müller, P. H. Vaccaro, F. Pérez-Bernal, and F. Iachello, J. Chem. Phys. **111**, 5038 (1999).
[26] A. Toniolo and M. Persico, J. Comput. Chem. **22**, 968 (2001).
[27] T. E. Sharp and H. M. Rosenstock, J. Chem. Phys. **41**, 3453 (1964).
[28] D. M. Burland and G. W. Robinson, J. Chem. Phys. **51**, 4548 (1969).
[29] I. Baraille, C. Larrieu, A. Dargelos, and M. Chaillet, Chem. Phys. **282**, 9 (2002).
[30] J. C. López, A. L. Rivera, Y. F. Smirnov, and A. Frank, Int. J. Quantum Chem. **88**, 280 (2002).
[31] T. Müller, P. H. Vaccaro, F. Pérez-Bernal, and F. Iachello, Chem. Phys. Lett. **329**, 271 (2000).
[32] K. Krantzman and D. Farrelly, Chem. Phys. Lett. **152**, 196 (1988).
[33] F. M. Fernández and J. F. Ogilvie, Chem. Phys. Lett. **169**, 292 (1990).
[34] E. J. Heller and D. Beck, Chem. Phys. Lett. **202**, 350 (1993).
[35] B. Segev and E. J. Heller, J. Chem. Phys. **112**, 4004 (2000).
[36] A. V. Sergeev and B. Segev, J. Phys. A **35**, 1769 (2002).
[37] S. Kallush, B. Segev, A. V. Sergeev, and E. J. Heller, J. Phys. Chem. A **106**, 6006 (2002).
[38] E. P. Wigner, Phys. Rev. **40**, 749 (1932).
[39] M. V. Berry, Philos. Trans. R. Soc. London, Ser. A **287**, 237 (1977).
[40] E. J. Heller, J. Chem. Phys. **68**, 2066 (1978).
[41] B. Hüpper and B. Eckardt, Phys. Rev. A **57**, 1536 (1998).
[42] E. J. Heller, B. Segev, and A. V. Sergeev, J. Phys. Chem. B **106**, 8471 (2002).
[43] R. K. Preston and J. C. Tully, J. Chem. Phys. **54**, 4297 (1971).
[44] M. F. Herman, J. Chem. Phys. **103**, 8081 (1995).
[45] M. F. Herman, J. Chem. Phys. **110**, 4141 (1999).
[46] M. F. Herman, J. Chem. Phys. **111**, 10427 (1999).
[47] M. Ben-Nun, J. Quenneville, and T. J. Martinez, J. Phys. Chem. A **104**, 5161 (2000).
[48] M. D. Hack, A. M. Wensmann, D. G. Truhlar, M. Ben-Nun, and T. J. Martinez, J. Chem. Phys. **115**, 1172 (2001).
[49] H. W. Lee, Phys. Rep. **259**, 147 (1995).
[50] A. Frank, A. L. Rivera, and K. B. Wolf, Phys. Rev. A **61**, 054102 (2000).
[51] P. M. Morse, Phys. Rev. **34**, 57 (1929).
[52] G. Pöschl and E. Teller, Z. Phys. **83**, 143 (1933).
[53] K. Weide and R. Schinke, J. Chem. Phys. **90**, 7150 (1989).